

Electronic supplementary information

Proton transport in oxalate compounds of iron(III) containing (alkyl)ammonium cations: The influence of the density of hydrogen bonds on conductivity

Ana Lozančić,^a Sanja Burazer,^a Sanja Renka,^a Krešimir Molčanov,^a Lidija Molčanov,^a and
Marijana Jurić^{a,*}

^a Ruđer Bošković Institute, Bijenička cesta 54, 10000 Zagreb, Croatia

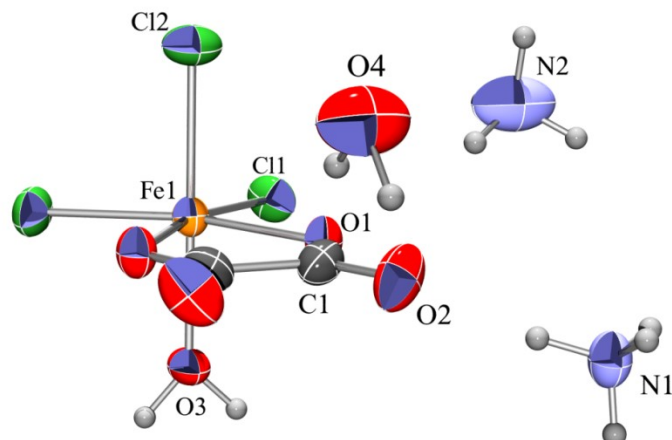


Fig. S1 ORTEP-3 drawing of a formula unit of compound $(\text{NH}_4)_2[\text{Fe}(\text{H}_2\text{O})\text{Cl}_3(\text{C}_2\text{O}_4)] \cdot \text{H}_2\text{O}$ (**1**) with atom numbering scheme. Displacement ellipsoids are drawn for the probability of 50 % and hydrogen atoms are shown as spheres of arbitrary radii.

Table S1 Selected distances (\AA) and angles ($^\circ$) for the coordination sphere of the iron(III) in compounds $(\text{NH}_4)_2[\text{Fe}(\text{H}_2\text{O})\text{Cl}_3(\text{C}_2\text{O}_4)] \cdot \text{H}_2\text{O}$ (**1**), $\{[\text{NH}(\text{CH}_3)_2(\text{C}_2\text{H}_5)][\text{FeCl}_2(\text{C}_2\text{O}_4)] \cdot \text{H}_2\text{O}\}_n$ (**2**) and $\{[\text{N}(\text{CH}_3)(\text{C}_2\text{H}_5)_3][\text{FeCl}_2(\text{C}_2\text{O}_4)]\}_n$ (**3**)

1	2	3			
Fe1–O1	2.045(4)	Fe1–O1	2.139(3)	Fe1–O2	2.050(8)
Fe1–O1 ^a	2.045(4)	Fe1–O2	2.067(3)	Fe1–O4	2.061(7)
Fe1–O3	2.102(5)	Fe1–O3	2.154(3)	Fe1–O3	2.148(8)
Fe1–Cl1 ^a	2.3280(15)	Fe1–O4 ⁱ	2.039(3)	Fe1–O1	2.158(7)
Fe1–Cl1	2.3280(15)	Fe1–Cl1	2.2424(10)	Fe1–Cl2	2.243(5)
Fe1–Cl2	2.3407(18)	Fe1–Cl2	2.2525(10)	Fe1–Cl1	2.243(4)
O1–Fe1–O1 ^a	78.71(16)	O1–Fe1–O2	78.01(11)	O2–Fe1–O4	158.3(3)
O1–Fe1–O3	87.03(17)	O1–Fe1–O3	80.12(11)	O2–Fe1–O3	86.0(3)
O1–Fe1–Cl1 ^a	167.96(12)	O2–Fe1–O4 ^b	86.41(12)	O2–Fe1–O1	78.2(3)
O1–Fe1–Cl1	90.34(11)	O1–Fe1–O4 ^b	84.64(11)	O2–Fe1–Cl2	100.6(3)
O1–Fe1–Cl2	93.28(10)	O2–Fe1–O3	158.78(11)	O2–Fe1–Cl1	93.5(3)
O1 ^a –Fe1–O3	87.03(17)	O3–Fe1–O4 ^b	78.51(11)	O4–Fe1–O3	77.8(3)
O1 ^a –Fe1–Cl1 ^a	90.34(11)	O1–Fe1–Cl1	89.44(9)	O4–Fe1–O1	84.8(3)
O1 ^a –Fe1–Cl1	167.96(12)	O1–Fe1–Cl2	167.97(9)	O4–Fe1–Cl2	93.2(2)
O1 ^a –Fe1–Cl2	93.28(10)	O2–Fe1–Cl1	98.78(9)	O4–Fe1–Cl1	100.7(2)
O3–Fe1–Cl1 ^a	87.42(12)	O2–Fe1–Cl2	92.53(8)	O3–Fe1–O1	79.8(3)
O3–Fe1–Cl1	87.42(12)	O3–Fe1–Cl1	168.13(8)	O3–Fe1–Cl2	167.9(3)
O3–Fe1–Cl2	179.60(19)	O3–Fe1–Cl2	91.72(8)	O3–Fe1–Cl1	90.0(2)
Cl1 ^a –Fe1–Cl1	100.09(6)	O4–Fe1–Cl1 ^b	95.34(9)	O1–Fe1–Cl2	91.6(2)
Cl1 ^a –Fe1–Cl2	92.32(5)	O4–Fe1–Cl12 ^b	100.71(9)	O1–Fe1–Cl1	167.2(3)
Cl1–Fe1–Cl2	92.32(5)	Cl1–Fe1–Cl2	99.44(4)	Cl2–Fe1–Cl1	99.58(18)

^aSymmetry operators: *i*) x , $1/2-y$, z

^bSymmetry operators: *i*) $-x$, $-y$, $2-z+2$.

Table S2 Hydrogen-bonding geometry in compounds $(\text{NH}_4)_2[\text{Fe}(\text{H}_2\text{O})\text{Cl}_3(\text{C}_2\text{O}_4)] \cdot \text{H}_2\text{O}$ (**1**) and $\{[\text{NH}(\text{CH}_3)_2(\text{C}_2\text{H}_5)][\text{FeCl}_2(\text{C}_2\text{O}_4)] \cdot \text{H}_2\text{O}\}$ (**2**)

Compound	D–H…A	D–H / \AA	H…A / \AA	D…A / \AA	D–H…A / $^\circ$	Symm. op. on A
1	N1–H1A…Cl1	0.95(8)	2.70(5)	3.413(6)	132.4(13)	$1+x, y, z$
	N1–H1B…O2	0.94(3)	2.47(5)	3.162(8)	131(3)	$2-x, -1/2+y, 2-z$
	N1–H1C…O1	0.94(4)	1.89(5)	2.820(6)	171(5)	x, y, z
	N2–H2A…O1	0.95(7)	2.40(7)	3.120(7)	132(6)	x, y, z
	N2–H2A…O2	0.95(7)	2.53(7)	3.469(9)	168(5)	x, y, z
	N2–H2C…O4	0.93(9)	1.95(10)	2.752(13)	143(10)	$1-x, -1/2+y, 1-z$
	O3–H3A…O1	0.93(6)	1.93(6)	2.800(4)	155(6)	$1-x, -y, 2-z$
	O4–H4A…Cl1	1.07	2.54	3.386(7)	135	$1+x, y, z$
	O4–H4A…Cl2	1.07	2.75	3.359(9)	116	$1+x, y, z$
2	O4–H4BA…O2	0.96(6)	2.41(4)	3.219(9)	142.6(17)	x, y, z
	O4–H4B…N2	0.96(6)	2.41(6)	2.752(13)	101(3)	$1-x, 1/2+y, 1-z$
	N1–H1…O5	0.98	1.79	2.755(4)	170	$1-x, 1-y, 1-z$
	O5–H5C…O1	0.94(5)	1.85(4)	2.747(4)	158(4)	$1+x, y, z$
	O5–H5D…Cl2	0.95(4)	2.52(4)	3.364(3)	148(4)	$1+x, y, z$
	O5–H5D…O5	0.95(4)	2.52(4)	3.364(3)	148(4)	$1+x, y, z$

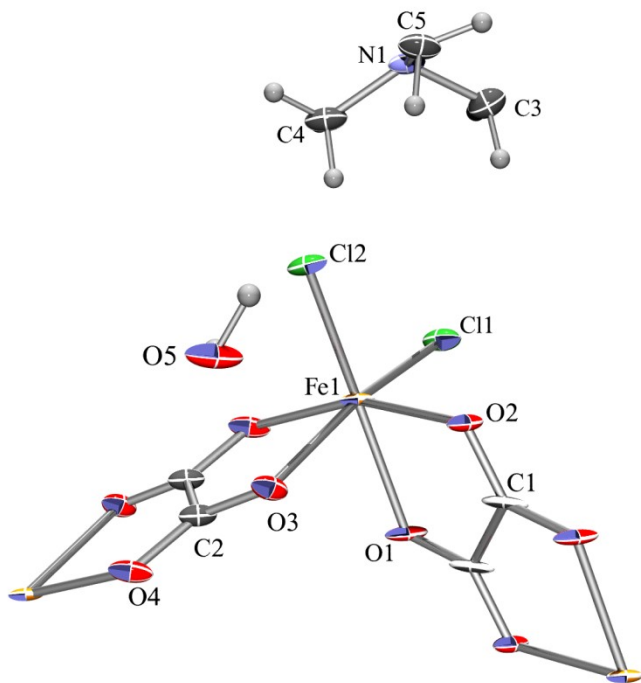


Fig. S2 ORTEP-3 drawing of a formula unit of compound $\{[\text{NH}(\text{CH}_3)_2(\text{C}_2\text{H}_5)][\text{FeCl}_2(\text{C}_2\text{O}_4)] \cdot \text{H}_2\text{O}\}_n$ (**2**) with atom numbering scheme. Displacement ellipsoids are drawn for the probability of 50 % and hydrogen atoms are shown as spheres of arbitrary radii.

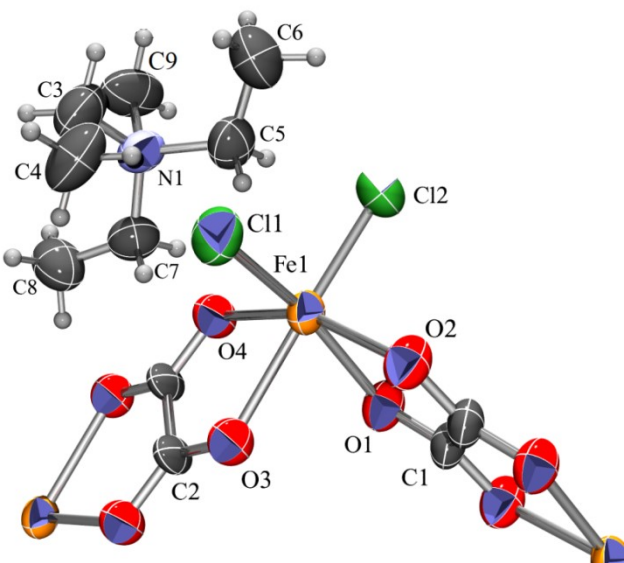


Fig. S3 ORTEP-3 drawing of a formula unit of compound $\{[N(CH_3)(C_2H_5)_3][FeCl_2(C_2O_4)]\}_n$ (**3**) at room temperature with atom numbering scheme. Displacement ellipsoids are drawn for the probability of 30 % and hydrogen atoms are shown as spheres of arbitrary radii.

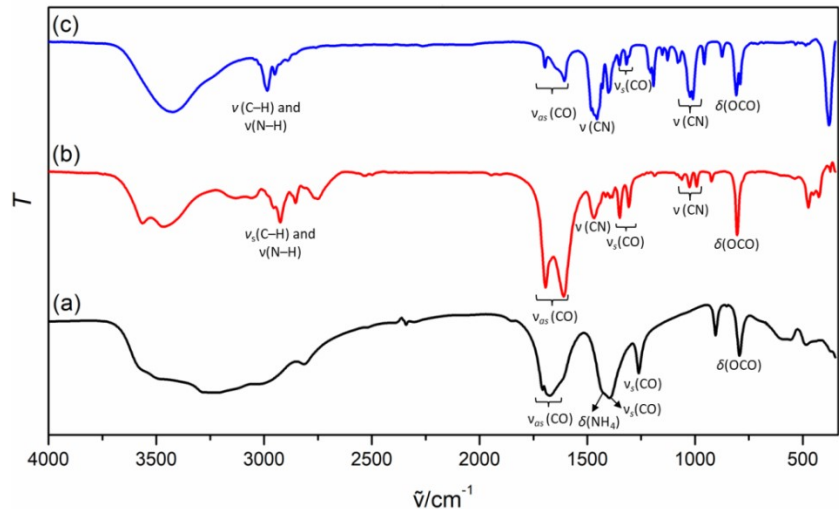
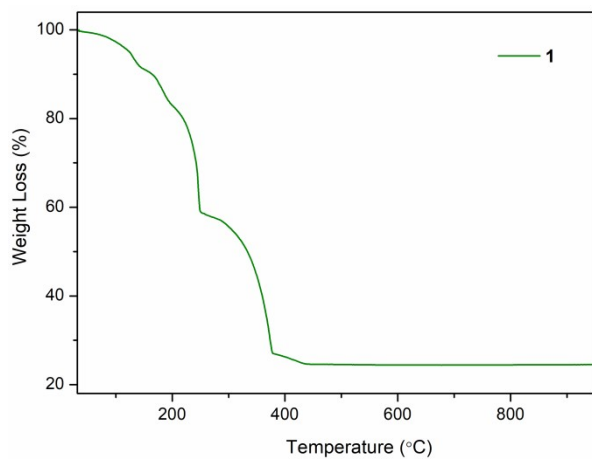


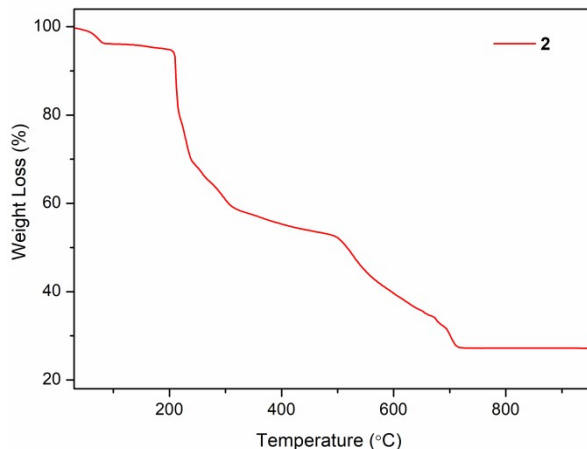
Fig. S4 Infrared spectra of compounds (a) $(\text{NH}_4)_2[\text{Fe}(\text{H}_2\text{O})\text{Cl}_3(\text{C}_2\text{O}_4)] \cdot \text{H}_2\text{O}$ (1) (b) $\{\text{NH}(\text{CH}_3)_2(\text{C}_2\text{H}_5)\}[\text{FeCl}_2(\text{C}_2\text{O}_4)] \cdot \text{H}_2\text{O}\}_n$ (2) and (c) $\{\text{N}(\text{CH}_3)(\text{C}_2\text{H}_5)_3\}[\text{FeCl}_2(\text{C}_2\text{O}_4)]\}_n$ (3).

Table S3 Selected absorption bands (cm^{-1}) of the oxalate groups in the infrared spectra of compounds 1–3

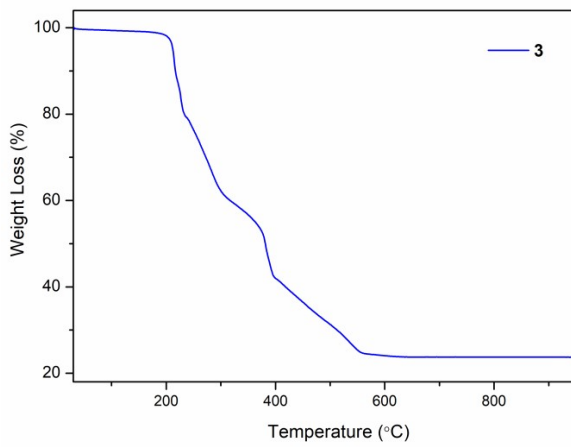
Comp.	Bidentate oxalate group			Bis(bidentate) oxalate group		
	$\nu_{as}(\text{CO})$	$\nu_s(\text{CO})$	$\delta(\text{OCO})$	$\nu_{as}(\text{CO})$	$\nu_s(\text{CO})$	$\delta(\text{OCO})$
1	1711	1397	794	—	—	—
	1681	1261	—	1694, 1609	1350, 1307	805
	1651	—	—	1697 1609	1350 1307	808
2	—	—	—	—	—	—
3	—	—	—	—	—	—



(a)



(b)



(c)

Fig. S5 TG curves for compounds (a) $(\text{NH}_4)_2[\text{Fe}(\text{H}_2\text{O})\text{Cl}_3(\text{C}_2\text{O}_4)] \cdot \text{H}_2\text{O}$ (**1**), (b) $\{[\text{NH}(\text{CH}_3)_2(\text{C}_2\text{H}_5)][\text{FeCl}_2(\text{C}_2\text{O}_4)] \cdot \text{H}_2\text{O}\}_n$ (**2**) and (c) $\{[\text{N}(\text{CH}_3)(\text{C}_2\text{H}_5)_3][\text{FeCl}_2(\text{C}_2\text{O}_4)]\}_n$ (**3**), measured in the synthetic air atmosphere.

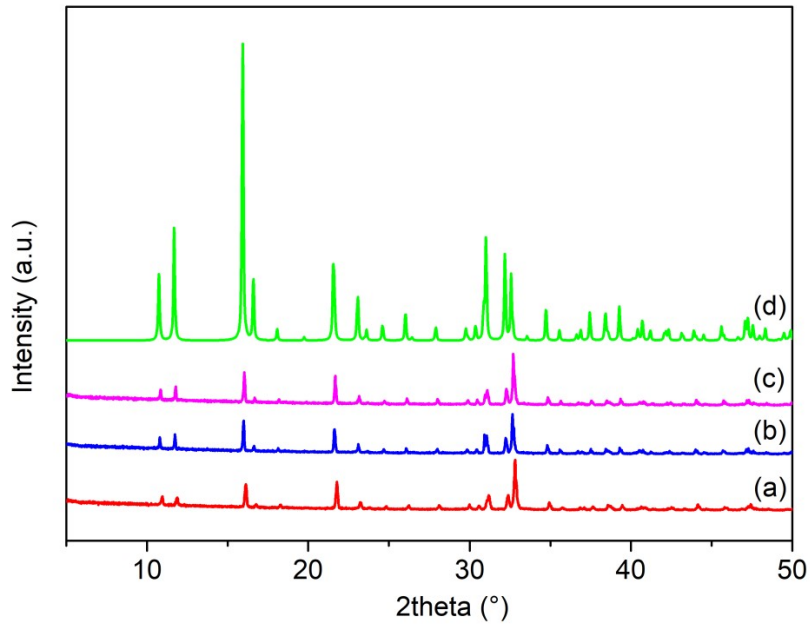


Fig. S6 Experimental PXRD patterns of compound $(\text{NH}_4)_2[\text{Fe}(\text{H}_2\text{O})\text{Cl}_3(\text{C}_2\text{O}_4)] \cdot \text{H}_2\text{O}$ (**1**): (a) before the humidity treatment, (b) after 2 hours of the humidity treatment (65% RH), (c) after 4 hours of the humidity treatment (65% RH), and (d) the simulated pattern from its single-crystal diffraction data.

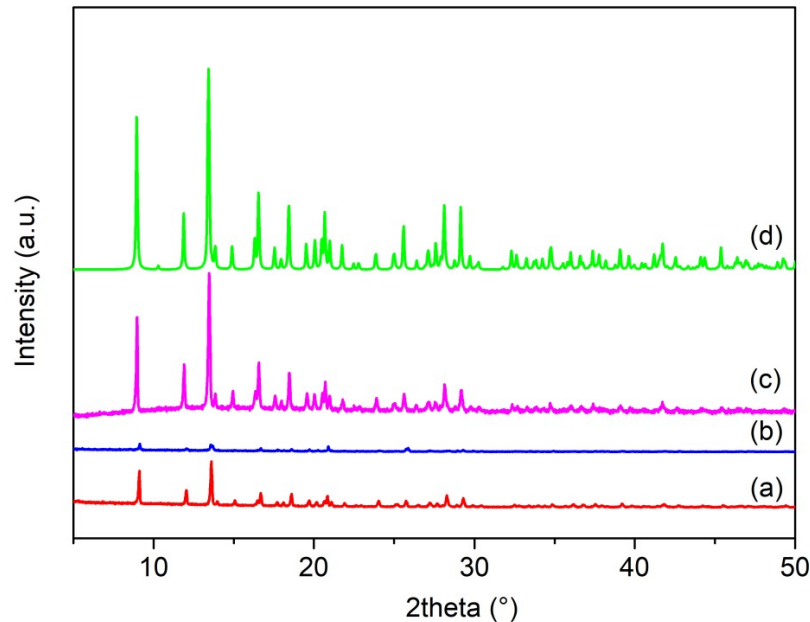


Fig. S7 Experimental PXRD patterns of compound $\{[\text{NH}(\text{CH}_3)_2(\text{C}_2\text{H}_5)][\text{FeCl}_2(\text{C}_2\text{O}_4)] \cdot \text{H}_2\text{O}\}_n$ (**2**): (a) before the humidity treatment, (b) after 2 hours of the humidity treatment (90% RH), (c) after 18 hours of the humidity treatment (90% RH), and (d) the simulated pattern from its single-crystal diffraction data.

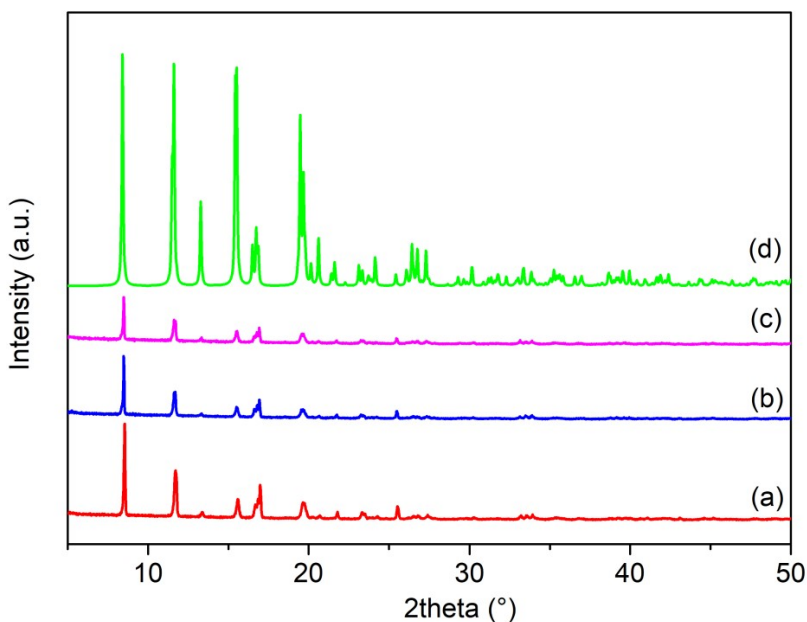


Fig. S8 Experimental PXRD patterns of compound $\{[N(CH_3)(C_2H_5)_3][FeCl_2(C_2O_4)]\}_n$ (**3**): (a) before humidity treatment, (b) after 2 hours of the humidity treatment (90% RH), (c) after 18 hours of the humidity treatment (90% RH), and (d) the simulated pattern from its single-crystal diffraction data.

Table S4 The values of electrical conductivity at different relative humidities for compounds **1–3** and compound from Ref. [29]

1		2		3		Compound 1 from Ref. [29]	
RH / %	$\sigma_{DC} / (\Omega \text{ cm})^{-1}$	RH / %	$\sigma_{DC} / (\Omega \text{ cm})^{-1}$	RH / %	$\sigma_{DC} / (\Omega \text{ cm})^{-1}$	RH / %	$\sigma_{DC} / (\Omega \text{ cm})^{-1}$
10	4.59×10^{-11}	10	1.69×10^{-10}	10	3.68×10^{-11}	61	1.48×10^{-9}
24	1.25×10^{-10}	46	4.81×10^{-10}	34	4.74×10^{-11}	75	1.05×10^{-6}
74	2.17×10^{-3}	75	1.45×10^{-6}	75	4.97×10^{-7}	80	7.59×10^{-6}
		84	2.98×10^{-5}	84	6.38×10^{-6}	84	2.24×10^{-5}
		93	2.00×10^{-4}	93	9.17×10^{-6}	93	2.70×10^{-4}